Taylor & Francis
Taylor & Francis Group

RESEARCH PAPER

🔓 OPEN ACCESS | Check for updates

Myeloid autophagy genes protect mice against fatal TNF- and LPS-induced cytokine storm syndromes

Ya-Ting Wang[a], Amy Sansone[b], Asya Smirnov[c], Christina L. Stallings[c], and Anthony Orvedahl [b,d]

[a]Center for Infectious Disease Research, Department of Basic Medical Sciences, Tsinghua University School of Medicine, Beijing, Haidian, China; [b]Department of Pediatrics, Washington University School of Medicine in St. Louis, St. Louis, MO, United States; [c]Department of Molecular Microbiology, Washington University School of Medicine in St. Louis, St. Louis, MO, United States; [d]Department of Pathology and Immunology, Washington University School of Medicine in St. Louis, St. Louis, MO, United States

ABSTRACT

Macroautophagy/autophagy regulates inflammation via multiple mechanisms, including lysosomal degradation of specific cellular components. Certain autophagy gene "cassettes" also participate in non-canonical processes to mediate important biological activities. While select autophagy genes in myeloid cells have been implicated in protecting mice in models of cytokine storm syndromes (CSS), a more extensive genetic analysis of the autophagy pathway for this disorder has not been reported to date. We determined that multiple canonical autophagy genes in the myeloid compartment protected against fatal disease from both intravenous TNF and intraperitoneal LPS, with the notable exception that *Atg14* was dispensable for the latter. Serum cytokine analyses and genetic crosses further revealed distinct mechanisms contribute to the hypersensitivity of autophagy gene-deficient mice in these CSS models. Surprisingly, TNF was dispensable for the increased mortality of myeloid *5*-deficient mice challenged with LPS. Tissue-specific ablation of *Atg5* in cells expressing ITGAX/CD11c and LYZ2/LYSM, but not S100A8/MRP8, defined a myeloid subset that protected against TNF, while protection against LPS was conferred by *Atg5* in a distinct subset of LYZ2-expressing cells. Together, this study identifies autophagy gene sets and specific cell types that protect against fatal inflammation due to CSS, highlighting important differences in two commonly used murine models of the disorder.

Abbreviations: ATG5: autophagy related 5; ATG7: autophagy related 7; ATG14: autophagy related 14; ATG16L1: autophagy related 16-like 1 (S. cerevisiae); BECN1: beclin 1, autophagy related; CASP1: caspase 1; CASP4/CASP11: caspase 4, apoptosis-related cysteine peptidase; CIM: conditionally immortalized macrophage; CLP: cecal ligation and puncture; CSS: cytokine storm syndrome; DC: dendritic cell; IFNG/IFNγ: interferon gamma; IFNGR1: interferon gamma receptor 1; ip: intraperitoneal; iv: intravenous; IL12/p70: interleukin 12, p70 heterodimer; IL18: Interleukin 18; ITGAX/CD11c: integrin alpha X; LAP: LC3-associated phagocytosis; LPS: lipopolysaccharide; LYZ2/LYSM: lysozyme 2; MAP1LC3A/LC3: microtubule-associated protein 1 light chain 3 alpha; RB1CC1/FIP200: RB1-inducible coiled-coil 1; S100A8/MRP8: S100 calcium binding protein A8 (calgranulin A); TICAM1/TRIF: TIR domain containing adaptor molecule 1; TLR4: toll-like receptor 4; TNF: tumor necrosis factor.

Introduction

Autophagy is a highly evolutionarily conserved process in which endogenous or foreign cytosolic material is enveloped within a double-membrane autophagosome and delivered to the lysosome for degradation [1]. Essential factors required for regulating various steps in autophagosome formation and lysosomal fusion have been identified and characterized in recent decades [1,2]. Though genetic deletion of many autophagy factors results in embryonic lethality, studies using mice with haploinsufficiency or tissue-specific genetic ablation have identified roles for autophagy-related genes in diverse health and disease states including regulation of immune responses [1,3,4]. Autophagy-related genes in myeloid cells are particularly important for the maintenance of immune homeostasis to regulate responses to viral and bacterial infections [5–9], preventing lupus-like auto-inflammatory disease [10], and survival in models of cytokine storm syndromes (CSS) [11–15].

The CSS refers to a state of increased systemic cytokine production with associated organ dysfunction triggered by various causes (reviewed in [16]). These include bacterial sepsis, hemophagocytic lymphohistiocytosis/macrophage activation syndrome, cytokine release syndrome from anti-tumor therapies, and viral infections, including coronavirus disease 2019/COVID-19 [17]. Conditions that model the sepsis-like CSS in mice include intravenous TNF (tumor necrosis factor; ivTNF) injection [18], intraperitoneal lipopolysaccharide (LPS; ipLPS), and cecal ligation and puncture (CLP) [19]. While these models have distinct features, the extent to which each model recapitulates different aspects of human disease remains an open question. Studies show that certain autophagy-related genes in
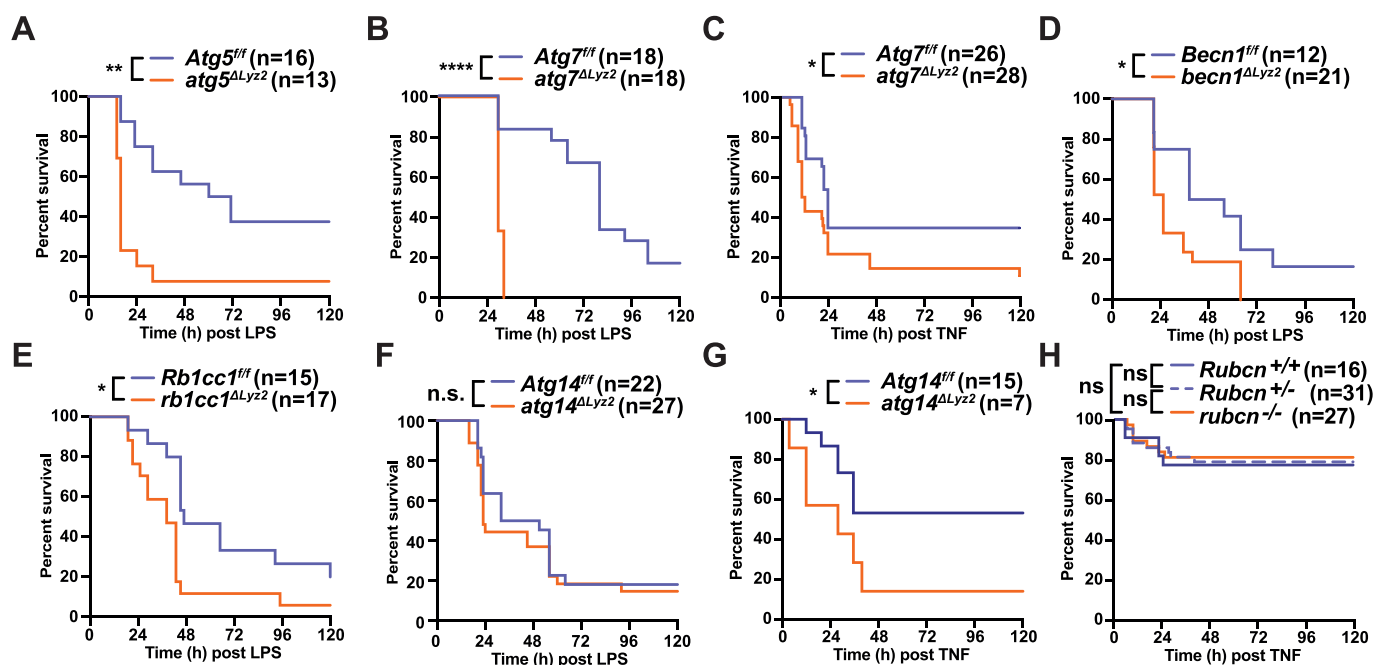

Figure 1. Select myeloid autophagy genes confer protection against fatal endotoxin and TNF-induced shock. (**A-H**) Survival of mice of indicated genotype in model indicated along x-axis. Data combined from the following number of mice: (**A**) Atg5^f/f (4F, 12 M), atg5^ΔLys2 (2F, 11 M), from 2 independent experiments; (**B**) Atg7^f/f (5F, 13 M), atg7^ΔLyz2 (9F, 9 M), from 2 independent experiments; (**C**) Survival of Atg7^f/f (8F, 18 M) or atg7^ΔLyz2 (8F, 20 M) mice, with 7.5 μg ivTNF, from 5 independent experiments. (**D**) Becn1^f/f (9F, 3 M), becn1^ΔLyz2 (9F, 12 M), from 3 independent experiments; (**E**) Rb1cc1^f/f (5F, 10 M), rb1cc1^ΔLyz2 (9F, 8 M), from 5 independent experiments; (**F**) Atg14^f/f (14F, 8 M), atg14^ΔLyz2 (18F, 9 M), from 4 independent experiments. (**G**) Survival of Atg14^f/f (4F, 11 M) or atg14^ΔLyz2 (5F, 2 M) mice, with 6 μg ivTNF, from 4 independent experiments. (**H**) Survival of Rubcn^+/+ (9F, 7 M), Rubcn^± (11F, 20 M), or rubcn^-/- (11F, 16 M) mice, with 7.5 μg ivTNF, from 7 independent experiments. p-values: *, <0.05; **, <0.01; ****, <0.0001; n.S., not significant; via Log-rank (Mantel Cox) test.

different tissues are important for protection against end-organ injury and/or mortality in each of these mouse models [11–30]. However, it is also now well-established that autophagy factors participate in diverse biological activities in addition to their roles in the canonical lysmortality in models of LPS-induced shockosomal-degradative pathway of macroautophagy [1,31]. Some of these processes include MAP1LC3A/LC3-associated phagocytosis (LAP) [10,32,33], BECN1 (beclin 1, autophagy related)-UVRAG-associated endocytosis [34], secretory processes [35,36], and cell death regulation [37,38]. We recently demonstrated myeloid-specific Atg5, Atg16l1, Rb1cc1/Fip200, and Becn1 are necessary to protect against ivTNF-induced fatal CSS, which indicates that canonical autophagy in myeloid cells protects against TNF toxicity [15]. However, the full extent to which canonical autophagy participates in regulating the CSS remains incompletely understood.

LPS derived from Gram-negative bacterial cell envelope is a potent pathogen associated molecular pattern that triggers inflammatory responses through TLR4 (toll-like receptor 4) signaling [39,40], and through non-canonical inflammasome sensing of intracellular LPS by CASP4/CASP11 (caspase 4, apoptosis-related cysteine peptidase) [41,42]. Intraperitoneal injection of LPS in mice results in dose-dependent mortality which requires both TLR priming and CASP4 sensing [41,42]. TNF also contributes to mortality in models of LPS-induced shock [43–51]. Because ivTNF can directly induce a form of fatal CSS on its own, whether ivTNF entails a distinct model of CSS or it recapitulates limited aspects of the ipLPS model is incompletely understood. This distinction has important implications, as multiple human sepsis trials investigating TNF

neutralization therapies have shown only marginal efficacy, and were based in part on promising results in pre-clinical animal models [52]. Therefore, a more complete understanding of host factors that regulate various pre-clinical CSS models could inform future clinical trials in humans.

Here we sought to systematically define the genetic determinants of the immunopathogenesis of murine CSS models with respect to the autophagy pathway. Given that many studies to date have investigated single autophagy-related genes in isolation during the ipLPS response, and that these genes have pleiotropic functions, we performed a detailed study on the role of multiple autophagy factors across several essential autophagy complexes between ivTNF and ipLPS models. We found that myeloid expression of Atg5, Atg7, Becn1, and Rb1cc1, but not Atg14, were important to protect against fatal disease from ipLPS. These findings contrast with ivTNF, for which we showed myeloid Atg14 conferred protection. Mice with myeloid-specific Atg5-deficiency (atg5^ΔLyz2) or Becn1-deficiency (becn1^ΔLyz2) exhibited dysregulated cytokines at baseline and after ivTNF, with elevated interferon gamma (Ifng/IFNγ) as a notable common finding. becn1^ΔLyz2 mice exhibited more markedly elevated cytokines in ipLPS compared to ivTNF. Together these findings illustrate both shared and unique functions of autophagy factors in different CSS models, and provide additional evidence that ivTNF and ipLPS model distinct aspects of the CSS. Intriguingly, increased mortality of atg5^ΔLyz2 with ipLPS is independent of TNF, which resembles outcomes in human sepsis. We also determined that a ITGAX/CD11c-expressing subset of myeloid cells was important for ATG5 to protect against ivTNF,

which differed from the cellular determinants of protection against ipLPS. Together these findings have important implications for understanding the CSS triggered by diverse etiologies and indicate select sets of autophagy genes may confer distinct protective mechanisms in different models.

Results

Select autophagy genes in myeloid cells protect against ipLPS and ivTNF

To evaluate the role of autophagy during CSS, we challenged mouse strains deficient for autophagy genes in myeloid cells with ipLPS and monitored them for survival. Similar to our findings with ivTNF [15], $atg5^{\Delta Lyz2}$ mice were markedly more susceptible to ipLPS compared to littermate $Atg5^{f/f}$ controls (Figure 1a). $atg7^{\Delta Lyz2}$ mice were also profoundly more sensitive to ipLPS, consistent with previous reports (Figure 1b [11,14]. Myeloid $Atg7$ was similarly required to protect against ivTNF (Figure 1c). These data, in combination with our previous studies, confirm an important role for components of the LC3-conjugation machinery, such as ATG5 and ATG7, in protection against both ivTNF and ipLPS. We next sought to determine if factors that regulate other steps of the autophagy pathway in myeloid cells also protect against ipLPS. BECN1 is required for nucleating nascent autophagosomal membranes and for autophagosome-lysosome fusion [34,53–56]. Similar to increased

mortality with ivTNF [15], $becn1^{\Delta Lyz2}$ mice exhibited increased mortality compared to their littermates injected with ipLPS (Figure 1d). We next tested if a LAP-independent process was involved in the response to ipLPS, as the LC3-conjugation machinery and BECN1 participate in LAP [10,32]. RB1CC1 is necessary for initiation of autophagosome formation during canonical autophagy [57,58], but is dispensable for LAP [32,59]. $rb1cc1^{\Delta Lyz2}$ mice were hypersensitive to ipLPS (Figure 1e), suggesting LAP-independent canonical autophagy genes protected against ipLPS, consistent with our previous findings for ivTNF [15]. To further evaluate the role of autophagy complexes, we challenged mice with myeloid deficiency of ATG14, a known interacting partner of BECN1 that plays an essential role for autophagosome nucleation and autophagosome-lysosome fusion [34,55,56,60,61]. Surprisingly, susceptibility of $atg14^{\Delta Lyz2}$ mice to ipLPS was indistinguishable from their littermates (Figure 1f). In contrast, $atg14^{\Delta Lyz2}$ mice were significantly sensitized to ivTNF (Figure 1g). RUBCN is essential for LAP [32], and has been shown to improve survival during ipLPS via germline deletion [24]. We found that deletion of $Rubcn$ had no effect on the susceptibility to ivTNF (Figure 1h). These results raised the possibility that a select subset of autophagy genes regulates ipLPS response, whereas a canonical set of autophagy genes mediates resistance to ivTNF. These results also provided genetic evidence that ivTNF and ipLPS are distinct models of CSS, the pathogenesis of which required different pathways to control.
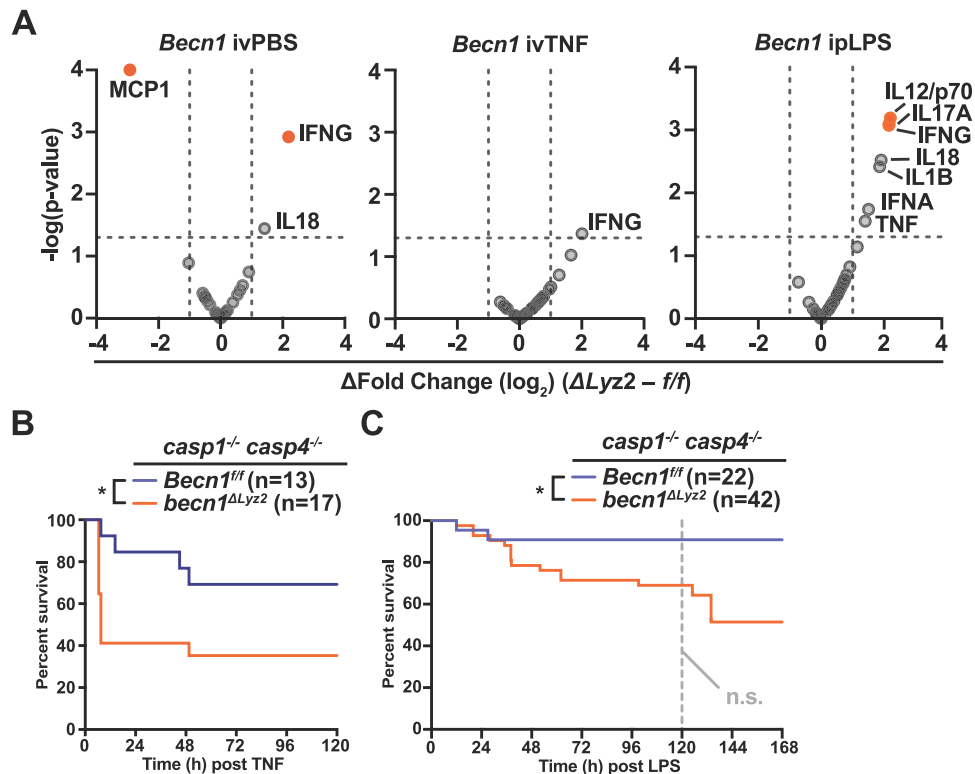

Figure 2. $becn1^{\Delta Lyz2}$ mice exhibit dysregulated cytokine responses and $Casp1$- and $Casp4$-independent mortality in CSS models. (**A**) Volcano plots showing differences ($becn1^{\Delta Lyz2}$ - $Becn1^{f/f}$) in serum cytokines of mice treated with ivPBS (left), ivTNF (middle), or ipLPS (right). "δfold Change" is the relative difference in fold change for the comparison indicated. Dashed lines: vertical = 2-fold change; horizontal = nominal p-value < = 0.05. Orange color reflects adjusted p-value < = 0.05. Relates to Figure S2A, which shows absolute fold changes for each cytokine and treatment compared to $Becn1^{f/f}$ treated with ivPBS. (**B-C**) Survival of mice of indicated genotype in ivTNF (B) and ipLPS (C) models. Data combined from the following number of mice: (B) $Becn1^{f/f}casp1^{-/-}casp4^{-/-}$ (6F, 7 M), $becn1^{\Delta Lyz2}casp1^{-/-}casp4^{-/-}$ (3F, 14 M), from 3 independent experiments; (C)$Becn1^{f/f}casp1^{-/-}casp4^{-/-}$ (11F, 11 M), $becn1^{\Delta Lyz2}casp1^{-/-}casp4^{-/-}$ (20F, 22 M), from 5 independent experiments. p-values: *, <0.05; n.s., not significant (at 120 h timepoint, dashed gray line); via Log-rank (Mantel Cox) test.

becn1ΔLyz2 mice exhibit dysregulated cytokine responses and partial Casp1- and Casp4-independent mortality in CSS

To further explore the role of autophagy-related genes and mechanism of hypersensitivity in CSS models, we assessed systemic cytokine production in $becn1^{\Delta Lyz2}$ mice with i.v. vehicle, ivTNF, or ipLPS via a 36-plex cytokine panel. $becn1^{\Delta Lyz2}$ mice exhibited significantly elevated IFNG levels compared to $Becn1^{f/f}$ mice with vehicle treatment alone (Figure 2a, S1). While ivTNF induced strong cytokine responses in both $becn1^{\Delta Lyz2}$ mice and their littermates (Fig. S1), only IFNG remained significantly elevated in $becn1^{\Delta Lyz2}$ mice compared to control mice after ivTNF. In contrast, ipLPS elicited marked elevation of cytokines including IL12/p70 and IL17A, in addition to IFNG in $becn1^{\Delta Lyz2}$ mice compared to control mice (Figure 2a, S1). Thus, $becn1^{\Delta Lyz2}$ mice exhibited dysregulated cytokines at baseline (which was previously observed in older mice [10]), and also upon challenge in CSS models.

We observed nominally elevated IL18 at baseline and with ipLPS, and elevated IL1B after ipLPS. This observation is consistent with previous reports indicating that autophagy in macrophages negatively regulates inflammasome-mediated production of these cytokines [11,26,27,62,63]. Both IL18 and IL1B are activated by CASP1 or CASP4, and have been implicated in the pathogenesis of ipLPS [64–70]. Therefore, to test the possibility that elaboration of IL18 and/or IL1B via these caspases contribute to hypersensitivity of $becn1^{\Delta Lyz2}$ mice in CSS models, we genetically ablated Casp1 and Casp4 in $becn1^{\Delta Lyz2}$ mice. In response to ivTNF, 69% of $Becn1^{f/f}casp1^{-/-}casp4^{-/-}$ mice survived to the endpoint (Figure 2b), compared to our previous results with 38% survival in $Becn1^{f/f}$ treated with the same ivTNF dose and route, and mice bred in the same facility [15]. This implied a relative protective effect of CASP1 and CASP4 deficiency with ivTNF, which is consistent with a previous report [69]. Despite improved survival under $casp1^{-/-}casp4^{-/-}$ background, $becn1^{\Delta Lyz2}casp1^{-/-}casp4^{-/-}$ mice remained significantly more susceptible to ivTNF compared to their $Becn1^{f/f}casp1^{-/-}casp4^{-/-}$ littermates (Figure 2b), suggesting that CASP1 and CASP4,

and the cytokines elaborated by these enzymes, are dispensable for the mortality of $becn1^{\Delta Lyz2}$ mice with ivTNF.

In the ipLPS model, $Becn1^{f/f}casp1^{-/-}casp4^{-/-}$ mice were significantly protected against ipLPS (Figure 2c, compare with Figure 1c), similar to the near complete resistance of the $casp1^{-/-}casp4^{-/-}$ parental strain (10/10 mice survived, data not shown) published previously [64–71]. While not statistically significant by the 120 h endpoint, significantly fewer $becn1^{\Delta Lyz2}casp1^{-/-}casp4^{-/-}$ mice survived ipLPS by 7 days post-injection (Figure 2c). Therefore, although relatively elevated levels of IL18 and IL1B were found in the serum of $becn1^{\Delta Lyz2}$ mice as noted, we concluded that the increased mortality of these mice to ipLPS is not fully due to CASP1 and CASP4 activities.

becn1ΔLyz2 mice exhibit Ifngr1-independent mortality to ipLPS, but Ifngr1-dependent cytokine responses in CSS models

We next sought to determine if IFNG signaling contributed to the pathogenesis of the ipLPS model with respect to myeloid Becn1 deficiency. We were encouraged in this hypothesis by the following: 1) $becn1^{\Delta Lyz2}$ mice exhibited elevated serum IFNG levels (Figure 2a); 2) genetic ablation of Ifngr1 (interferon gamma receptor 1) rescues the hypersensitivity of $becn1^{\Delta Lyz2}$ mice to ivTNF [15]; and, 3) IFNG is known to contribute to mortality in LPS-induced shock [43,45,68,72–75]. To test this possibility, we fixed a germline $ifngr1^{-/-}$ mutation on $becn1^{\Delta Lyz2}$ mice and their littermates. Compared to mice with intact IFNG signaling (Figure 1c), mice on the $ifngr1^{-/-}$ background were relatively resistant to ipLPS (Figure 3a), similar to parental $ifngr1^{-/-}$ mice (10/12 mice survived, consistent with prior reports [45,68,75]). However, $becn1^{\Delta Lyz2}ifngr1^{-/-}$ mice remained significantly sensitized to fatal ipLPS-induced disease despite ablation of IFNG-signaling (Figure 3a).

Given that IFNG provides a key stimulus to activate macrophage cytokine production (reviewed in [76]), but has a distinct role in ivTNF compared to ipLPS, we sought to determine the cytokine responses that IFNG elicits in $becn1^{\Delta Lyz2}$ mice compared to $becn1^{\Delta Lyz2}ifngr1^{-/-}$ mice. Although IFNG was dysregulated in $becn1^{\Delta Lyz2}$ mice, the
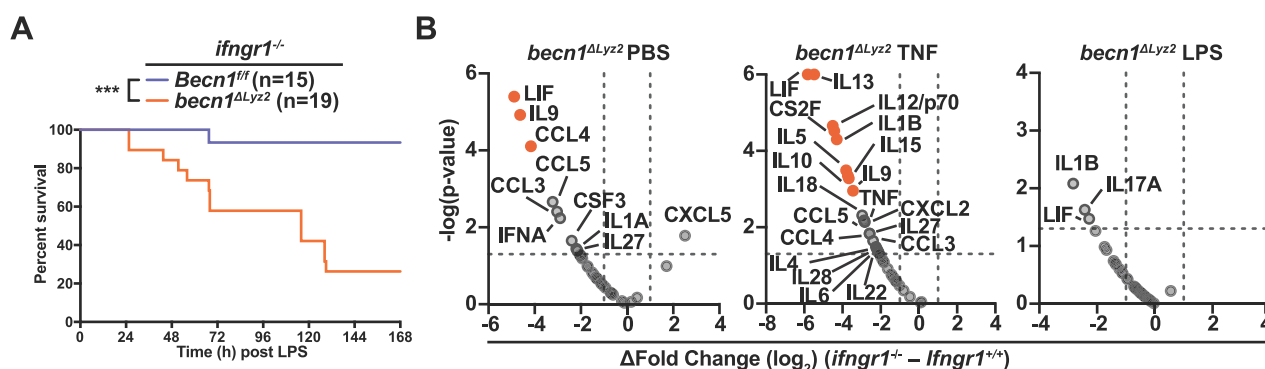
Figure 3. $becn1^{\Delta Lyz2}$ mice exhibit Ifngr1-independent mortality to ipLPS, but Ifngr1-dependent cytokine responses in CSS models. (**A**) Survival of mice of indicated genotype with ipLPS in the following numbers: $Becn1^{f/f}$ $ifngr1^{-/-}$ (6F, 9 M), $becn1^{\Delta Lyz2}ifngr1^{-/-}$ (6F, 13 M), from 3 independent experiments. p-values: (at 120 h **, <0.01), ***, <0.001; via Log-rank (Mantel Cox) test. (**B**) Volcano plots showing differences (($becn1^{\Delta Lyz2}ifngr1^{-/-}$) – ($Becn1^{f/f}$ $Ifngr1^{+/+}$)) in serum cytokines of mice treated with ivPBS (left), ivTNF (middle), or ipLPS (right). "δfold Change" is the difference in fold change for the comparison indicated, relative to $Becn1^{f/f}$ $Ifngr1^{+/+}$ treated with ivPBS for all conditions (as in Fig. 2). Dashed lines: vertical = 2-fold change; horizontal = nominal p-value < = 0.05. Orange color reflects adjusted p-value < = 0.05.

cytokine itself was not affected by the absence of its receptor (Figure 3b). However, in sham treated animals and those injected with ivTNF, a significant reduction in multiple cytokines was observed in $becn1^{\Delta Lyz2}$ mice lacking $Ifngr1$ compared to those with intact IFNG signaling (Figure 3b). Only nominal reductions were observed in select cytokines (IL1B, IL17B, and LIF) in the ipLPS model (Figure 3b). Therefore, combined with our previous findings that IFNG signaling is required for the hypersensitivity of $becn1^{\Delta Lyz2}$ mice to ivTNF [15], we concluded that a dysregulated IFNG-TNF axis is responsible for increased susceptibility of $becn1^{\Delta Lyz2}$ to ivTNF, whereas the hypersensitivity of $becn1^{\Delta Lyz2}$ mice to ipLPS is largely independent of IFNG.

atg5ΔLyz2 mice exhibit markedly dysregulated cytokine responses in CSS models and TNF-independent hypersensitivity to ipLPS

Given that BECN1 participates in pleiotropic cellular activities, we next sought to determine if the dysregulated IFNG-TNF axis observed in $becn1^{\Delta Lyz2}$ mice was recapitulated by deletion of another autophagy-related gene, $Atg5$. Myeloid $Atg5$ deficiency resulted in elevation of numerous cytokines compared to their littermates at baseline with ivPBS (Figure 4a, S2). The most significantly and robustly elevated cytokine in $atg5^{\Delta Lyz2}$ mice was IFNG, which was also true for $becn1^{\Delta Lyz2}$ mice at baseline. After ivTNF treatment, several cytokines, including IFNG were elevated in $atg5^{\Delta Lyz2}$ mice compared to their littermates (Figure 4a, right). Together, these data show that mice with autophagy gene-deficiency exhibit elevated inflammatory cytokines at baseline, with evidence for dysregulation along an IFNG-TNF axis.

We next sought to determine the role of TNF in the ipLPS model, as it was elevated at baseline in $atg5^{\Delta Lyz2}$ mice (Figure 4a and Fig. S2), and it has been implicated in the pathogenesis of the ipLPS murine model either via genetic ablation or therapeutic neutralization [43–51,77]. Therefore, we hypothesized that TNF may contribute to the hypersensitivity of $atg5^{\Delta Lyz2}$ mice to ipLPS. Similar to previous findings in wildtype mice [43,44,50,78], we found $Atg5^{f/f}$ animals

treated with TNF neutralizing antibodies prior to ipLPS were nearly completely protected against fatal disease compared to those that received isotype control antibodies (Figure 4b). In stark contrast, $atg5^{\Delta Lyz2}$ littermates remained markedly sensitized to ipLPS with no protection conferred by TNF neutralization (Figure 4b). These results suggest that while TNF mediates ipLPS sensitivity in wild-type mice, ipLPS toxicity in $atg5^{\Delta Lyz2}$ mice is independent of TNF.

Atg5 in distinct myeloid compartments protects against ivTNF and ipLPS

ATG5 in myeloid cells limits the basal inflammatory tone, which impacts infection due to influenza A virus and *Mycobacterium tuberculosis*, as shown via LYZ2-specific deletion [5,7]. LYZ2-cre deletes genes in multiple myeloid subsets that mainly include macrophages, monocytes, dendritic cells (DCs), and neutrophils [79]. To date, information on the specific myeloid cell types in which ATG5 exerts its immune regulatory roles is limited. During *Mycobacterium tuberculosis* infection, S100A8-expressing neutrophils lacking $Atg5$ are responsible for the immunopathological phenotype seen in $atg5^{\Delta Lyz2}$ mice [7]. Therefore, we sought to further delineate the myeloid subtypes that are important for $Atg5$ to protect against CSS. First, we confirmed that $Atg5$ is efficiently deleted in purified macrophage and DC subsets in multiple tissues in mice with $Atg5$ deficiency driven by $Itgax$-cre ($atg5^{\Delta Itgax}$) (Fig. S3). As expected, $Atg5$ was most efficiently deleted in $Itgax$-expressing DCs and lung macrophages in these mice. $atg5^{\Delta Itgax}$ mice were more susceptible to ivTNF (Figure 5a). In contrast, $Atg5$ deletion in neutrophils ($atg5^{\Delta S100A8}$) had no effect on the susceptibility to ivTNF (Figure 5b), although $Atg5$ was effectively deleted in neutrophils of these mice as previously confirmed using the same breeding colony [7]. Intriguingly, loss of $Atg5$ from either neutrophils or DCs was insufficient to phenocopy $atg5^{\Delta Lyz2}$ mice with ipLPS (Figure 5 c and d). Therefore, we concluded that ATG5 activity in $Itgax$-expressing cells but not neutrophils mediates resistance to ivTNF in mice, while ATG5 in $Itgax$-negative macrophages protects against ipLPS. These results further underscored that
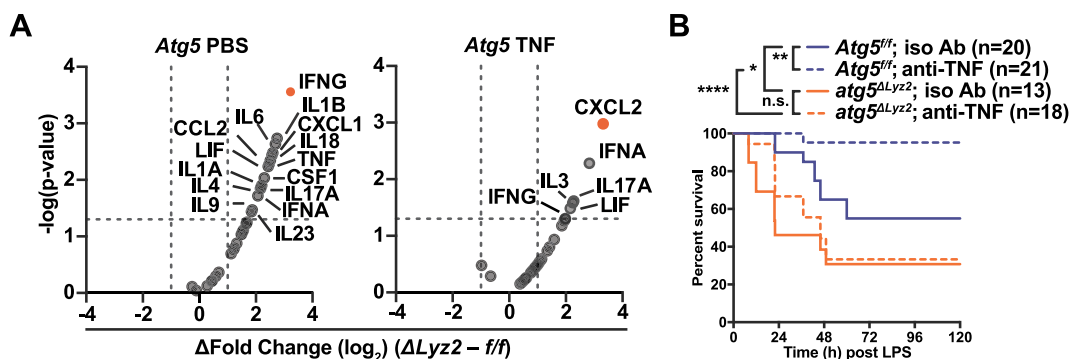

Figure 4. $atg5^{\Delta Lyz2}$ mice exhibit dysregulated cytokines at baseline and with ivTNF, and TNF-independent mortality to ipLPS. (**A**) Volcano plots showing differences ($atg5^{\Delta Lyz2}$ – $Atg5^{f/f}$) treated with ivPBS (left), or ivTNF (right). "δfold Change" is the relative difference in fold change for the comparison indicated, relative to $Atg5^{f/f}$ treated with ivPBS. Figure S2 shows absolute fold changes for each cytokine and treatment. (**B**) Survival of mice of indicated genotype and treatment with ipLPS in the following numbers: $Atg5^{f/f}$ iso Ab (11F, 9 M), $Atg5^{f/f}$ anti-TNF (8F, 13 M), $atg5^{\Delta Lyz2}$ iso Ab (4F, 9 M), $atg5^{\Delta Lyz2}$ anti-TNF (6F, 12 M), from 4 independent experiments. p-values: *, <0.05; **, <0.01; ****, <0.0001; n.S., not significant; via Log-rank (Mantel Cox) test. "iso Ab", isotype control antibody; "anti-TNF", TNF-neutralizing antibody.
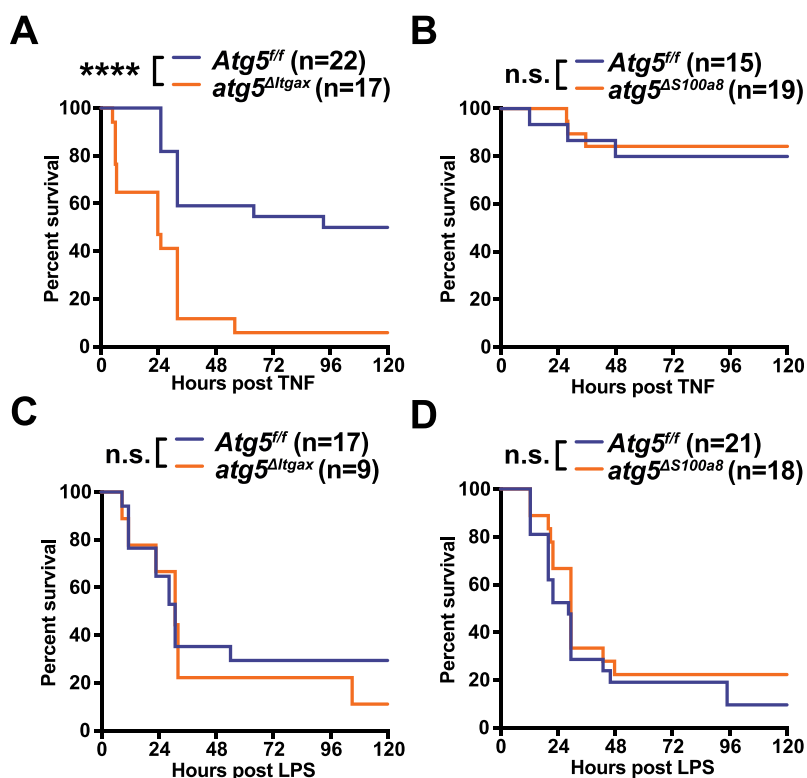
Figure 5. *Atg5* exhibits cell compartment-specific protective effects with ivTNF and ipLPS. Survival of mice of indicated genotype with ivTNF (**A** and **B**) or ipLPS (**C** and **D**), in the following numbers: (A) *Atg5^f/f^* (12F, 10 M), *atg5^ΔItgax^* (8F, 9 M), from 4 independent experiments; (B) *Atg5^f/f^* (10F, 5 M), *atg5^ΔS100a8^* (7F, 12 M), from 5 independent experiments; (C) *Atg5^f/f^* (7F, 10 M), *atg5^ΔItgax^* (1F, 8 M), from 5 independent experiments; (D) *Atg5^f/f^* (14F, 7 M), *atg5^ΔS100a8^* (9F, 9 M), from 4 independent experiments. *p*-values: ****, <0.0001; n.S., not significant; via Log-rank (Mantel Cox) test.

CSS model-specific phenotypes exist with respect to the role of autophagy-genes in specific myeloid cells.

Atg5, Becn1, and Atg14 exert select effects on cytokine production, but confer extensive protection against cell death

To evaluate the role of autophagy in macrophages in response to IFNG, TNF, and LPS, we turned to conditionally immortalized bone marrow-derived macrophages (CIMs). CIMs have been shown to recapitulate primary bone marrow-derived macrophages with respect to the role of autophagy in immunity [80]. We focused on IL18 and IL12/p70 responses, which were elevated in myeloid autophagy-deficient mice (Figures 2a, 4a, and S1). IL18 is constitutively expressed but requires inflammasome for activation and secretion (reviewed in [81]), while IL12/p70 is produced via the canonical secretory pathway (reviewed in [82]). We first confirmed that the autophagy-related genes targeted were efficiently deleted in differentiated LYZ2-Cre expressing CIMs (Fig. S4). While we observed induction of IL12/p70 with LPS and potentiation with IFNγ, we observed significantly less production in *ΔLyz2* cells from *Becn1* and *Atg14* mice, as opposed to increased levels (Figure 6a–c). We observed less robust induction of IL18, and only significant increases in cells lacking *Becn1* after stimulation with LPS (Figure 6d–f). These data suggest that hypercytokinemia

observed in myeloid autophagy-deficient mice may not be due to macrophage-intrinsic effects of autophagy, and that multicellular interactions underlie the pathogenesis of cytokine storm in vivo. Concurrently, additional factors may be necessary for hyper-production of these cytokines in autophagy-deficient macrophages in vivo. Concentrations of TNF and LPS used in these stimulation experiments were sufficient to provoke macrophage responses, as we observed death of CIMs via live cell imaging (Figure 6g–i). We previously found that multiple canonical autophagy genes in BV2 macrophage-like cell line, and *Atg5* in bone marrow-derived macrophages, confer protection against IFNG/TNF-induced cell death [15]. Similar to *Atg5*, loss of either *Becn1* or *Atg14* also markedly sensitized cells to TNF- and IFNG-induced death compared to *f/f* cells (Figure 6g–i). Similarly, while IFNG synergized with LPS to induce death of *f/f* cells, both or either stimuli induced significantly more pronounced cell death in *Atg5*, *Becn1*, or *Atg14* deficient macrophages (Figure 6g–i). These data provide genetic evidence that canonical autophagy confers a cytoprotective effect to macrophages in response to IFNG, TNF, and LPS. However, the activity of autophagy in promoting cell survival can only partially explain our in vivo findings, as increased cell death in *Atg14* deficient cells is not consistent with the equivalent susceptibility to ipLPS challenge (Figure 1f), and IFNG signaling is dispensable for the hypersusceptibility of *becn1^ΔLyz2^* mice to ipLPS (Figure 3a).
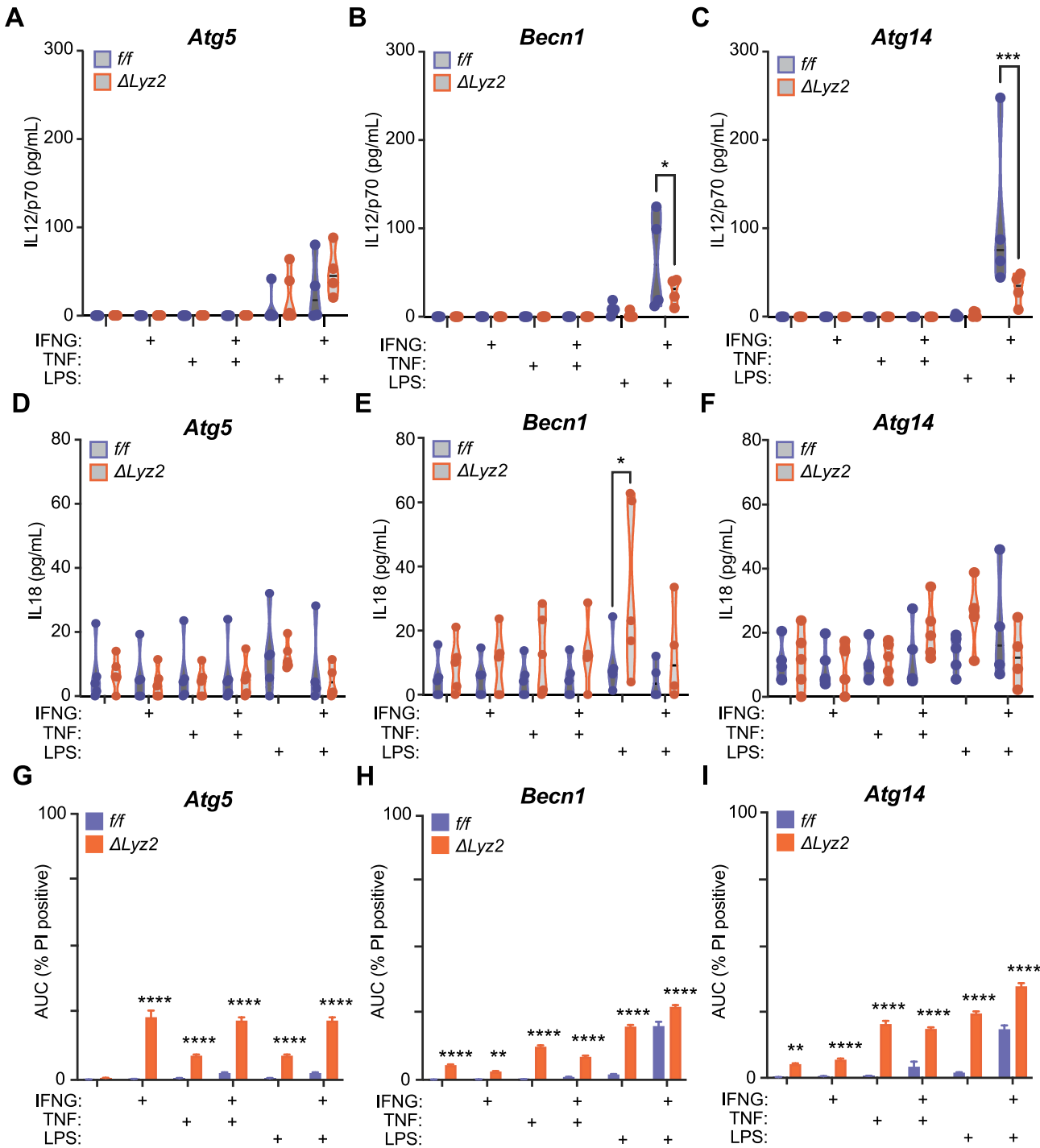
Figure 6. Cytokine production and cell death in macrophages from autophagy-gene deficient mice. Cytokine concentrations (Il12/p70 in (**A-C**) or IL18 in (**D-F**)) in supernatants, and cell death (**G-I**), of macrophages differentiated from $Atg5^{f/f}$ and $atg5^{\Delta Lyz2}$ mice (A, D, G), $Becn1^{f/f}$ and $becn1^{\Delta Lyz2}$ mice (B, E, H), or $Atg14^{f/f}$ and $atg14^{\Delta Lyz2}$ mice (C, F, I). Cells in A-F stimulated as indicated for 24 hours. Percent death in (G-I) represents AUC measurement over 64 h time course, where 100% represents no live cells for duration of experiment. *p*-values: ***, <0.001; ****, <0.0001; $\delta lyz2$ vs. *f/f* for each treatment (2-way ANOVA, Sidak's multiple comparison test). Each point in A-F represent average values from 4–5 independent experiments. Data in G-I represent mean + SEM with similar results observed in 3 independent experiments.

Discussion

Regulation of inflammation by maintenance of cellular homeostasis is increasingly recognized as an essential function of autophagy genes. In this study, we sought to dissect the role of autophagy-related genes in protection against two distinct models of the CSS. We extended the known number of genes in myeloid cells necessary for protecting against ivTNF [15], and found a similar genetic requirement protecting against ipLPS, with the exception of *Atg14* being dispensable for ipLPS. These results inform the selection of
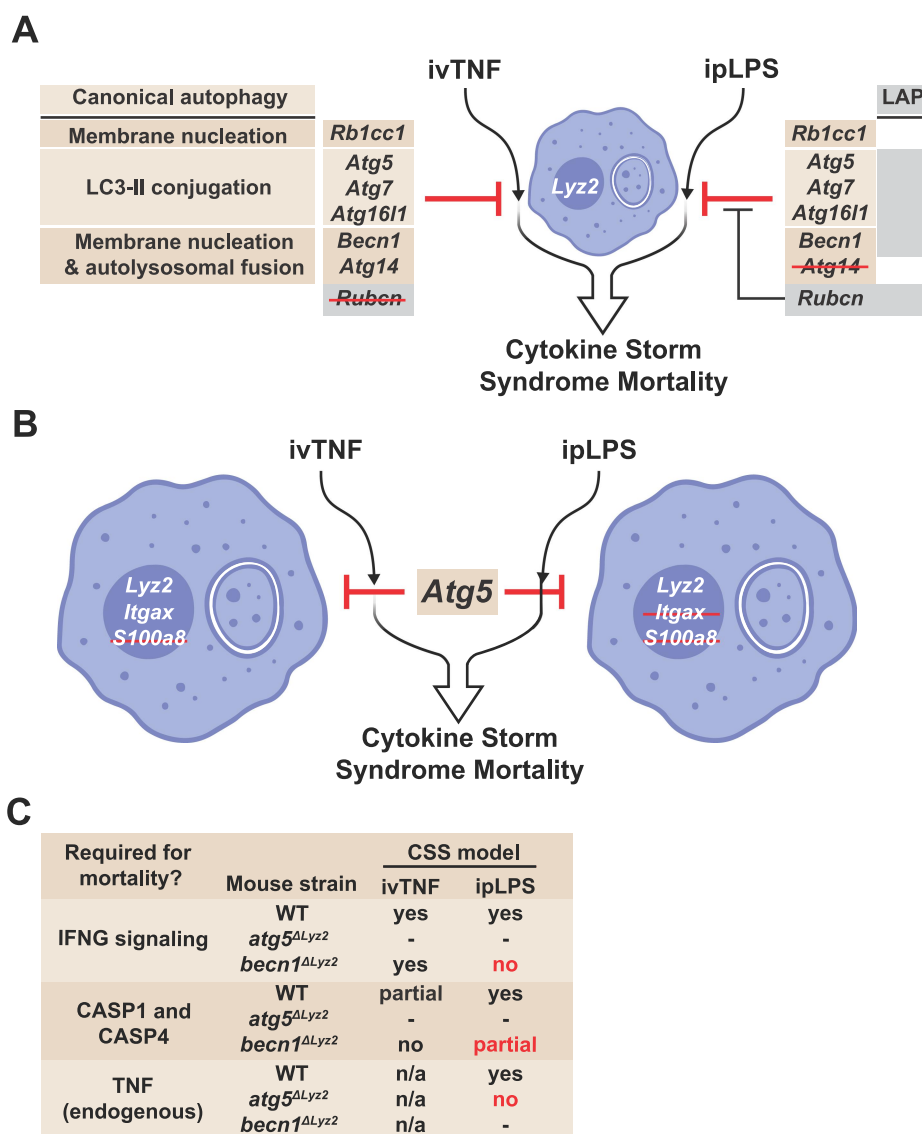
Figure 7. Summary of myeloid autophagy gene regulation of CSS. (**A**) Involvement of autophagy related genes in LYZ2+ cells, or role of germline *Rubcn* expression (reported here and in [24]) in LC3-associated phagocytosis (LAP), in either TNF or LPS models and their role in autophagy regulation. (**B**) Role of ATG5 in subsets of LYZ2+ myeloid cells in TNF or LPS models. (**C**) Role of specific mediators of mortality or effects of *atg5* deletion (Δ) in TNF or LPS models, with key differences highlighted in red text. "-", indicates not tested in current study; "n/a", not applicable to model tested.

preclinical models of CSS in the study of autophagy factors. Our findings are summarized in the model shown in Figure 7, and they give rise to hypotheses as to the protective mechanism of myeloid autophagy-related genes. Table S1 summarizes studies to date on autophagy-related genes in models of sepsis-like CSS, including the results reported here. Importantly, while autophagy deficient mice exhibit evidence for a dysregulated IFNG-TNF axis, the activity of these cytokines was dispensable for hypersusceptibility to ipLPS. The differences observed here between the ivTNF and ipLPS models underscore the paradigm that these stimuli model non-redundant features of the CSS.

The dispensability of myeloid *Atg14* for survival of mice during ipLPS raises a number of key questions. To our knowledge, this is the only phenotype that has been reported to date involving genes encoding the LC3 conjugation machinery (e.g., *Atg5*, *Atg7*), *Becn1*, and *Rb1cc1*, but not *Atg14*. The ipLPS result with *Atg14* is unexpected given an emerging

model that genes regulating canonical autophagic lysosomal degradation of innate immune signaling scaffolds underlies protective effects of these genes (reviewed in [83]). For example, ATG16L1 is important for degrading TICAM1/TRIF (TIR domain containing adaptor molecule 1) and other RIP homotypic interaction motif/RHIM domain-containing proteins via the selective autophagy adaptor TAX1BP1 (Tax1 binding protein 1) in cultured macrophages [12,13]. However, it is not yet known if this molecular mechanism is responsible for the in vivo protection conferred by *Atg16l1* against ipLPS. Autophagy degrades inflammasome machinery [63] and limits triggering of the NLRP3 (NLR family pyrin domain containing 3) inflammasome by mitochondrial DNA [11,27], and inflammasome activity is elevated in autophagy gene deficient cells [26,62]. Though inflammasome activity was proposed as the mechanism of hypersusceptibility to ipLPS in autophagy deficient mice [11,26,27], the role of the inflammasome in the hypersusceptible phenotype remains incompletely

understood. Taking these studies together, the activity of TICAM1/TRIF in priming CASP4 for LPS responses provides one plausible mechanism for the reported hypersensitivity of autophagy deficient mice [84,85]. However, most studies to date associating autophagy and degradation of these LPS activated complexes with ipLPS mortality have focused on either LC3 itself [26,27], the LC3 conjugation machinery [11–13], or an LC3-associated receptor protein (SQSTM1/p62) [11]. Importantly, germline deficiency of RUBCN, which is required for LAP, confers a protective effect against ipLPS [24]. Taken together, our finding of the dispensable role of *Atg14* during ipLPS supports a hypothesis that a noncanonical LC3-associated autophagy-related process in myeloid cells counteracts a TICAM1/TRIF-CASP4 axis in mice with ipLPS.

Our study confirmed an important, though only partial, role for inflammasome activity in the hypersensitivity of $becn1^{\Delta Lyz2}$ mice to ipLPS. Given the marked resistance to high doses of ipLPS exhibited by $casp4^{-/-}$ mice [42,71], this suggests an as of yet unidentified pathway may be responsible for mortality of $becn1^{\Delta Lyz2}$ $casp1^{-/-} casp4^{-/-}$ mice. Conversely, $becn1^{\Delta Lyz2}$ mice lacking *Casp1* and *Casp4* remained hypersusceptible to ivTNF, confirming that caspase activity is dispensable for ivTNF-induced shock, further highlighting distinctions between these models. Previous studies support the notion of multifactorial pathophysiology in CSS. For example, IL1A and TNF synergize in mice to induce fatal CSS [47]. IL18 and IL1B combined deficiency confers resistance to lethal doses of LPS, but not to the same degree as $casp1^{-/-} casp4^{-/-}$-deficient mice with supra-lethal doses [69]. Along these lines, neutralization of IL18 or antagonism of IL1 receptor individually does not extinguish the hypersensitivity to ipLPS in $atg7^{\Delta Lyz2}$ mice [14]. It is not clear if combined neutralization of IL18 and IL1 receptor activity would rescue autophagy deficient mice, but our results with $casp1^{-/-} casp4^{-/-}$ mice suggest the effect might be incomplete. Interestingly, genetic ablation of $casp1^{-/-} casp4^{-/-}$ demonstrates a minor role in CLP and ivTNF models, while mice with combined deficiency in IL1B and IL18 exhibit complete protection in these models [69]. We found $atg5^{\Delta Lyz2}$ mice were hypersusceptible to both ivTNF and ipLPS, but the mortality to ipLPS in these mice was independent of TNF. Together these findings suggest that loss of autophagy-related genes may activate a novel pathway and/or enable redundancy between CASP1- and CASP4-elicited cytokines and TNF. It remains possible that IFNG and CASP1- and CASP4-elicited cytokines exert non-overlapping roles in the pathogenesis of ipLPS in autophagy-deficient mice, and deletion in combination could result in complete protection. Finally, a recent study indicated a model in which interferons and TNF from hematopoietic cells prime intestinal epithelial cells for CASP4- and CASP8-mediated cell death and tissue injury in lethal ipLPS model [86]. The effect of myeloid autophagy on limiting CASP8-mediated cell extrinsic responses remains to be determined.

Our study provides additional insight into the differing roles of myeloid autophagy genes in protection against ivTNF and ipLPS. The dispensability of *Atg14* in ipLPS but not ivTNF could indicate that different autophagy gene sets are important in select subsets of cells targeted by LYZ2. Given that LPS is administered intraperitoneally, it is possible that *Atg14* is less important in peritoneal macrophages for initiating the pathology but is required in another macrophages lineage that responds to ivTNF. Consistent with this, deletion of *Atg5* in a ITGAX-expressing compartment was sufficient to sensitize to ivTNF, but not ipLPS, while deletion of *Atg5* in the S100A8-expressing compartment did not recapitulate $atg5^{\Delta Lyz2}$ in either ivTNF or ipLPS models. This could help explain differences between ivTNF and ipLPS, for example since LYZ2 and ITGAX expression define certain macrophage subsets, such as alveolar macrophages, and ivTNF might primarily affect these cells. ipLPS might not access the same cell compartment directly, thus explaining the absence of phenotype in $atg5^{\Delta Itgax}$ mice in this model. However, ipLPS has systemic effects including robust induction of circulating TNF, such that cell compartment specificity does not fully explain the differences observed for $atg14^{\Delta Lyz2}$ and $atg5^{\Delta Lyz2}$ mice. The role of a select set of autophagy genes in regulating baseline activation profiles of myeloid cells was recently described, in which loss of *Becn1*, *Rb1cc1*, or *Atg14* resulted in hyperactivation of multiple macrophage populations in mice, and conferred resistance to *Listeria monocytogenes* [6]. Intriguingly, disruption of genes encoding the LC3 conjugation machinery *Atg5*, *Atg7*, and *Atg16l1*, did not result in hyperactivated macrophage phenotype [6]. Additionally, macrophage activation and *Listeria* resistance due to *Becn1* deletion mapped to a LYZ2 + compartment that did not involve S100A8- or ITGAX-expressing cells [6]. Here we demonstrated that hypersensitivity to ivTNF occurred with *Atg5* deletion in a LYZ2+ and ITGAX+ compartment, while susceptibility to ipLPS required a LYZ2+ compartment that did not require either S100A8- or ITGAX-expressing cells. Together, these studies indicate that specific sets of autophagy genes define resistance or susceptibility to infectious and inflammatory triggers with selectivity for different myeloid sub-compartments. It is important to note that our findings with *Atg5* in ITGAX-expressing cells may be due to noncanonical activities as we did not investigate additional autophagy genes in this compartment. Further studies with additional tissue-specific conditionally-null mice or cell reconstitution experiments in specific compartments will be important to define the physiological myeloid cell population(s) in which autophagy genes confer protection in different models of infection and CSS.

Our study has implications for pre-clinical models of human CSS. Previous studies implicate polymorphisms in *Irgm1* (immunity-related GTPase family M member 1; encodes an effector of antimicrobial autophagy) [87], *Atg16l1* [88], and *Atg5* [89] in severity of disease in sepsis. It has also been suggested that impaired autophagolysosomal activity in patients with chronic granulomatous disease may underlie their susceptibility to developing CSS [90]. This notion implicates canonical lysosomal degradative autophagy in association with disease severity in patients with CSS. It remains to be determined if these associations are pathogenic, or if the polymorphisms result in a gain or loss of gene function, but they raise the possibility that modulating

autophagy levels could be therapeutic in patients with CSS. However, given that *Atg14* was dispensable for ipLPS induced mortality in our study, the potential also exists that therapies targeting a sub-routine of the autophagy pathway may be more efficacious than inducers of canonical autophagy in certain forms of CSS. Our finding that TNF is dispensable for the hypersensitivity of *atg5*$^{\Delta Lyz2}$ mice to ipLPS correlates to a recent study in which reconstitution of the wild mouse microbiome abrogated the role of TNF in ipLPS [91]. Defining the mechanisms underlying TNF-independent mouse sepsis models could improve pre-clinical approaches to sepsis therapies. Similarly, canonical autophagy regulation of the IFNG-TNF axis specifically may have implications for alternative forms of CSS in which TNF does mediate a pathogenic role. Potential examples of this include highly pathogenic influenza or Severe Acute Respiratory Syndrome virus pulmonary infection, for which TNF neutralization is protective in murine models [92–94]. In contrast to the equivocal results of neutralizing TNF in human sepsis, modulation of the IFNG-TNF axis directly or via autophagy modulation have yet to be tested in trials for these other clinical scenarios.

Materials and methods

Mice

All mice used in this study have been described previously: *Atg5*$^{f/f}$ [95], *Atg7*$^{f/f}$ [96], *Atg16l1*$^{f/f}$ [97], *Atg14*$^{f/f}$ [55], *Rb1cc1/Fip200*$^{f/f}$ [98], *Becn1*$^{f/f}$ [99], *rubcn*$^{-/-}$ [32], *Lyz2/LysM*-cre (*ΔLyz2* herein; Jax, 004781) [100], *Itgax/CD11c*-cre (*Δitgax* herein; Jax, 007567) [101], *S100a8/MRP8*-cre (*ΔS100a8* herein; Jax 021614) [102], *casp1*$^{-/-}$ *casp4*$^{-/-}$ (Jax, 016621) [67], and *ifngr1*$^{-/-}$ (Jax, 003288) [103]. Mice were housed in a temperature-controlled specific-pathogen-free barrier vivarium with an alternating 12 h: 12 h light: dark cycle. For ivTNF survival experiments, mice were injected with TNF (PeproTech, 315-01A) in DPBS (Fisher, 14,190,144)-0.1% BSA (endotoxin-free; Fisher, 507,533,139) via lateral tail vein at 7.5 µg/mouse unless otherwise indicated in a final volume of 150–200 µL. Control animals were injected i.v. with PBS-0.1% BSA. For the ipLPS model, LPS/endotoxin from *E. coli* O55:B5 (Sigma, L2880) was solubilized in PBS at 2 mg/mL by heating for 10 min at 56°C and vortexing, three times, then injected intraperitoneally at a final dose of 20 mg/kg for all experiments. For TNF neutralization experiments, mice were injected i.p. with TNF neutralizing antibody (clone TN3–19.2; Leinco, T258) or isotype control antibody (PIP; Leinco, I-140) at a dose of 250 µg/mouse in PBS 72 h prior to LPS injection. Mice were monitored every 6–12 h for clinical signs of morbidity and euthanized if unable to ambulate to hydrogel food, unable to maintain upright posture, or if the core temperature nadir was <26°C using rectal thermometer for rodents (Bioseb). For cytokine analysis, mice were injected as above and euthanized with isofluorane and cervical dislocation 4 h post-injection. Serum was separated from whole blood collected in EDTA coated syringes by centrifugation at 2000 rcf × 10 min at 4°C. All mice were 8-12-weeks old at time of

injections. All experimental protocols were reviewed and approved by the Washington University Institutional Animal Care and Use Committee.

Cell lines

Bone marrow-derived macrophages were generated as described previously and samples prepared as per sorted cells [15]. HOXB8 bone marrow-derived progenitors of CIMs were independently generated from mice of the indicated genotype (Flox/Flox Cre-negative ("*f/f*"), or Flox/Flox/LYZ2-Cre-positive ("*ΔLyz2*")) for each strain, as described [104]. Briefly, bone marrow was harvested from cleaned femurs and tibia by flushing, or centrifuging cleaned bones in a 600-µl tube within a 1.5-mL tube at 15,000 rcf as described [105,106]. Progenitor cells were purified by negative selection with MACS lineage depletion (Miltenyi, 130-090-858). Progenitors were pre-stimulated in RPMI1640 (Gibco, 11,875,135), 15% FBS, 1% PSQ (pen-strep-glutamine [pen-strep, Gibco, 15,140–122; L-glutamine, Corning, 25-005-Cl), IL3 (10 ng/mL; PeproTech, 213–13), IL6 (20 ng/mL; PeproTech, 216–16), and KITL/SCF (25 ng/mL; PeproTech, 250–03) for 3 days prior to transduction. 250,000 cells were transduced by supernatants from Plat-E cells transfected with ER-HOXB8 retrovirus. HOXB8 progenitor media (RPMI1640, 10% FBS, 1% PSQ [Gibco, 10,378,016], 20 ng/mL murine CSF2/GM-CSF (Peprotech, 315–03), 1 µM β-estradiol (in ethanol, diluted 1:10,000 final; Sigma, E2758)) was added after 24 h, and cells were passaged in fresh HOXB8 media every 2–3 days until suspension cells were growing logarithmically and negative control wells had minimal viable cells. To differentiate CIMs for experiments, HOXB8 progenitor cells were pelleted, washed in PBS, then resuspended in CIM differentiation media (DMEM (High Glucose; Gibco, 11,960,077), 10% FBS, 10% CMG14–12 conditioned media (as described [97]), 1x glutamine (Fisher, 35,050,079), 1x sodium pyruvate (Fisher, 11,360,070)) and allowed to differentiate in untreated tissue culture flasks for 5–7 days. CIMs were harvested by scraping in ice cold 2 mM EDTA in PBS, washed, counted, and seeded for experiments in CIM differentiation media, and allowed to rest 1–3 days prior to stimulation.

Cytokine analysis

Serum samples were analyzed with the Mouse Chemokine/Cytokine Panel 1A (ThermoFisher, EPX360 -26,092-901) on a Luminex xMAP FlexMAP3D (Luminex Corp) with MilliporeSigma Belysa software. Fold change was calculated as follows: ((MFI for each sample – background) +1)/mean value of *floxed* control animals injected with PBS for each mouse strain. Normalization was performed within each Luminex run. Comparison of log$_2$ normalized fold changes was performed with *t*-test for Cre+ (Cre-positive) vs. Cre[a] (Cre-negative) for each cytokine and treatment. Statistical significance for multiple comparisons was determined by the Holm-Sidak method. ELISAs for IL18 (R&D Systems,

DY7625–05) and IL12/p70 (R&D Systems, DY419–05) were performed according to manufacturer's instructions, and developed signal quantified on a Varioskan Lux plate reader using SkanIt Software (v4.1.0.43) (Thermo Fisher).

Facs sorting

Mice were euthanized with isofluorane and cardiac-perfused with PBS. Tissue leukocytes collection was performed as previously described [6]. Briefly, peritoneal cells were collected from mice after injection of 5 ml of DMEM containing 2 mM EDTA and 2% FBS into the peritoneal space. Blood was collected by submandibular bleeding into EDTA tubes. Lungs and spleens were excised, placed in DMEM containing 10% FBS, minced finely and digested at 37°C for 1 h with mechanical disruption using a stir bar and enzymatic digestion. Lungs were digested with Liberase Blendzyme III (Liberase TM replacement; Sigma, 5,401,119,001), hyaluronidase (Sigma, H4272) and DNase I (Sigma, 11,284,932,001); spleens with collagenase B (Roche, 11,088,815,001) and DNase I. Cells were treated with ACK buffer (Gibco, A1049201) to remove red blood cells and were passed through a 70-μm cell strainer to generate single-cell suspension. Cells were stained in PBS with 2 mM EDTA and 3% FBS, with anti-FCGR2B /FcγRII-FCGR3/FcγRIII antibodies (BioLegend, 101,302) for blocking and with specific antibodies for labeling before sorting. Antibodies used for labeling were as follows: Peritoneal cells: CSF1 R/CD115 (eBioscience, 46-1152-80), ICAM2/ CD102 (BioLegend, 105,606), ADGRE1/F4/80 (eBioscience, 123,110), CD226 (BioLegend, 128,805), LY6 G/Ly-6 G (BioLegend, 127,613), I-A/I-E/MHC-II (BioLegend, 107,631), ITGAM/CD11b (BioLegend, 101,227). Blood leukocytes using ITGAX/CD11c (BioLegend, 117,306), CD19 (bdbiosciences, 552,854), CD3 (bdbiosciences, 552,774), LY76/Ter119 (BioLegend, 116,222), LY6 G, LY6C/Ly-6C (BioLegend, 128,026), PTPRC/CD45 (BioLegend, 103,128), MHC-II, ITGAM/CD11b. Lung cells using ITGAX/CD11c, ITGAM/ CD11b, MERTK (eBioscience, 12-5751-82), LY6 G, FCGR1/ CD64, PTPRC/CD45, MHC-II, SIGLECF (bdbiosciences, 740,388). Spleen using ITGAX/CD11c, CD4 (BioLegend, 100,540), ADGRE1/F4/80, CD3, CD19, LY6 G, CD8 (BioLegend, 100,714), PTPRC/CD45, MHC-II, ITGAM/ CD11b. Gating of tissue/blood cell populations was performed as described previously [6]. Cell sorting was performed on an FACSAria III Cell Sorter (BD Biosciences), and data were analyzed using FlowJo software (Tree Star). Collected cell pellets were snap frozen in 100% Ethanol in a dry ice bath and stored at −80°C until further analysis.

Analysis of Cre-mediated gene excision

Genomic DNA from cell pellets was extracted per manufacturer instructions with a Quick-DNA Microprep Plus kit (Zymo, D4074). Atg5 flox allele excision was determined by PCR as described previously [95]. BECN1 levels were analyzed via western blot as described [15]. Atg14 flox allele deletion was determined from gDNA amplified by PCR with the following primers: WT-5F: ttgaccgtcacagggtgtgagtgactt; WT-3 R: aagcagagttaggcttccctggtagaa; FLOX-5F: cccatctccattcctggattactggac;

and FLOX-3 R: ctaaagcgcatgctccagactgccttg. Wildtype allele without flox sequences produces a 600bp band with WT-5F and WT-3 R primers; floxed allele results in 450 bp band with FLOX-5F and FLOX-3 R primers; and excised allele results in 950 bp band with FLOX-5F and WT-3 R primers. Products were amplified with 95°C melt (×5 min), 95°C (×15 sec), 65°C (×1 min), 72°C (×1 min) for 30 cycles.

Cell death analysis

CIM cells were seeded in 96-well plates at a density of 30e4 total cells/well and allowed to rest for 2–3 days. Media was exchanged with fresh CIM media to normalize volumes, and cells were stimulated as indicated in the presence of Propidium Iodide (1 μg/mL final) and imaged on a Cytation 5 (Biotek) as described [15].

Software and statistical analyses

Statistical analyses were performed in Prism with posttest analyses indicated for each figure (v8.0.0.0, GraphPad Software, Inc.). Live cell imaging was acquired and analyzed with Gen 5 (v3.10, Biotek). Final figures were prepared in Adobe Illustrator (24.1.2) in which scales were uniformly adjusted for all data representations. Figure 7 generated in part with BioRender.com.

Disclosure statement

No potential conflict of interest was reported by the author(s).

ORCID

Anthony Orvedahl http://orcid.org/0000-0002-2481-9200

References

[1] Levine B, Kroemer G Biological functions of autophagy genes: a disease perspective. Cell. 2019;176:11–42.

[2] Mizushima N The exponential growth of autophagy-related research: from the humble yeast to the Nobel Prize. Febs Lett. 2017;591(5):681–689.

[3] Deretic V, Levine B Autophagy balances inflammation in innate immunity. Autophagy. 2018;14:243–251.

[4] Cadwell K Crosstalk between autophagy and inflammatory signalling pathways: balancing defence and homeostasis. Nat Rev Immunol. 2016;16:661–675.

[5] Lu Q, Yokoyama CC, Williams JW, et al. Homeostatic control of innate lung inflammation by vici syndrome gene epg5 and additional autophagy genes promotes influenza pathogenesis. Cell Host & Microbe. 2016;19:102–113.

[6] Wang Y-T, Zaitsev K, Lu Q, et al. Select autophagy genes maintain quiescence of tissue-resident macrophages and increase susceptibility to Listeria monocytogenes. Nat Microbiol. 2020;5:272–281.

[7] Kimmey JM, Huynh JP, Weiss LA, et al. Unique role for ATG5 in neutrophil-mediated immunopathology during M. tuberculosis infection. Nature. 2015;528:565–569.

[8] Park S, Buck MD, Desai C, et al. Autophagy genes enhance murine gammaherpesvirus 68 reactivation from latency by preventing virus-induced systemic inflammation. Cell Host & Microbe. 2016;19:91–101.

[9] Castillo EF, Dekonenko A, Arko-Mensah J, et al. Autophagy protects against active tuberculosis by suppressing bacterial burden and inflammation. Proceedings of the National Academy of Sciences of the United States of America 2012;109:E3168–76.

[10] Martinez J, Cunha LD, Park S, et al. Noncanonical autophagy inhibits the autoinflammatory, lupus-like response to dying cells. Nature. 2016;533(7601):115–119. DOI:10.1038/nature17950

[11] Zhong Z, Umemura A, Sanchez-Lopez E, et al. NF-κB restricts inflammasome activation via elimination of damaged mitochondria. Cell. 2016;164:896–910.

[12] Samie M, Lim J, Verschueren E, et al. Selective autophagy of the adaptor TRIF regulates innate inflammatory signaling. Nat Immunol. 2018;19:246–254.

[13] Lim J, Park H, Heisler J, et al. Autophagy regulates inflammatory programmed cell death via turnover of RHIM-domain proteins. Elife. 2019;8:10.

[14] Fattah EA, Bhattacharya A, Herron A, et al. Critical role for IL-18 in spontaneous lung inflammation caused by autophagy deficiency. J Immunol. 2015;194(11):5407–5416.

[15] Orvedahl A, McAllaster MR, Sansone A, et al. Autophagy genes in myeloid cells counteract IFNγ-induced TNF-mediated cell death and fatal TNF-induced shock. Proceedings of the National Academy of Sciences of the United States of America 2019;116:16497–16506.

[16] Behrens EM, Koretzky GA Review: cytokine storm syndrome: looking toward the precision medicine era. Arthritis Rheumatol. 2017;69:1135–1143.

[17] McGonagle D, Sharif K, O'Regan A, et al. The role of cytokines including interleukin-6 in COVID-19 induced pneumonia and macrophage activation syndrome-like disease. Autoimmun Rev. 2020;19:102537.

[18] Cauwels A, Janssen B, Waeytens A, et al. Caspase inhibition causes hyperacute tumor necrosis factor–induced shock via oxidative stress and phospholipase A2. Nat Immunol. 2003;4(4):387–393.

[19] Stortz JA, Raymond SL, Mira JC, et al. Murine models of sepsis and trauma: can we bridge the gap? Ilar J. 2017;58:90–105.

[20] Amir M, Zhao E, Fontana L, et al. Inhibition of hepatocyte autophagy increases tumor necrosis factor-dependent liver injury by promoting caspase-8 activation. Cell Death Differ. 2013;20:878–887.

[21] Lalazar G, Ilyas G, Malik SA, et al. Autophagy confers resistance to lipopolysaccharide-induced mouse hepatocyte injury.

[22] Mei S, Livingston M, Hao J, et al. Autophagy is activated to protect against endotoxic acute kidney injury. Sci Rep. 2016;6:10–22171.

[23] Sun Y, Yao X, Zhang Q-J, et al. Beclin-1-Dependent autophagy protects the heart during sepsis. Circulation. 2018;138:2247–2262.

[24] Zi Z, Song Z, Zhang S, et al. Rubicon deficiency enhances cardiac autophagy and protects mice from lipopolysaccharide-induced lethality and reduction in stroke volume. J Cardiovasc Pharmacol. 2015;65:252–261.

[25] Aguirre A, López-Alonso I, González-López A, et al. Defective autophagy impairs ATF3 activity and worsens lung injury during endotoxemia. J Mol Med. 2014;92(6):665–676. DOI:10.1007/s00109-014-1132-7

[26] Zhang Z, Xu X, Ma J, et al. Gene deletion of gabarap enhances Nlrp3 inflammasome-dependent inflammatory responses. J Immunol. 2013;190(7):3517–3524.

[27] Nakahira K, Haspel JA, Rathinam VAK, et al. Autophagy proteins regulate innate immune responses by inhibiting the release of mitochondrial DNA mediated by the NALP3 inflammasome. Nat Immunol. 2011;12(3):222–230. DOI:10.1038/ni.1980

[28] Oami T, Watanabe E, Hatano M, et al. Blocking liver autophagy accelerates apoptosis and mitochondrial injury in hepatocytes and reduces time to mortality in a murine sepsis model. Shock. 2018;50:427–434.

[29] Lo S, Yuan S-S, Hsu C, et al. Lc3 over-expression improves survival and attenuates lung injury through increasing autophagosomal clearance in septic mice. Ann Surg. 2013;257(2):352–363.

[30] Lin C-W, Lo S, Hsu C, et al. T-Cell autophagy deficiency increases mortality and suppresses immune responses after sepsis. PLoS One. 2014;9(7):e102066. DOI:10.1371/journal.pone.0102066

[31] Münz C The macroautophagy machinery in endo- and exocytosis. J Mol Biol. 2017;429:473–485.

[32] Martinez J, Malireddi RKS, Lu Q, et al. Molecular characterization of LC3-associated phagocytosis reveals distinct roles for Rubicon, NOX2 and autophagy proteins. Nat Cell Biol. 2015;17(7):893–906. DOI:10.1038/ncb3192

[33] Martinez J, Almendinger J, Oberst A, et al. Microtubule-Associated protein 1 light chain 3 alpha (LC3)-associated phagocytosis is required for the efficient clearance of dead cells. Proceedings of the National Academy of Sciences of the United States of America 2011;108:17396–17401.

[34] Itakura E, Kishi C, Inoue K, et al. Beclin 1 forms two distinct phosphatidylinositol 3-kinase complexes with mammalian Atg14 and UVRAG. Mol Biol Cell. 2008;19:5360–5372.

[35] Keller MD, Ching KL, Liang F-X, et al. Decoy exosomes provide protection against bacterial toxins. Nature. 2020;579:260–264.

[36] Leidal AM, Huang HH, Marsh T, et al. The LC3-conjugation machinery specifies the loading of RNA-binding proteins into extracellular vesicles. Nat Cell Biol. 2020;22:187–199.

[37] Pyo J-O, Jang M-H, Kwon Y-K, et al. Essential roles of Atg5 and FADD in autophagic cell death: dissection of autophagic cell death into vacuole formation and cell death. J Biol Chem. 2005;280:20722–20729.

[38] Seo J, Seong D, Nam YW, et al. Beclin 1 functions as a negative modulator of MLKL oligomerisation by integrating into the necrosome complex. Cell Death Differ. 2020;162:17–21.

[39] Hoshino K, Takeuchi O, Kawai T, et al. Cutting edge: toll-like receptor 4 (TLR4)-deficient mice are hyporesponsive to lipopolysaccharide: evidence for TLR4 as the Lps gene product. J Immunol. 1999;162(7):3749–3752.

[40] Poltorak A, He X, Smirnova I, et al. Defective LPS signaling in C3H/HeJ and C57BL/10ScCr Mice: mutations in Tlr4 gene. Science. 1998;282(5396):2085–2088. DOI:10.1126/science.282.5396.2085

[41] Hagar JA, Powell DA, Aachoui Y, et al. Cytoplasmic LPS activates caspase-11: implications in TLR4-independent endotoxic shock. Science. 2013;341:1250–1253.

American Journal of Physiology Gastrointestinal and Liver Physiology 2016; 311:G377–86.

[42] Kayagaki N, Wong MT, Stowe IB, et al. Noncanonical inflamma-some activation by intracellular LPS independent of TLR4. Science. 2013;341:1246–1249.

[43] Doherty GM, Lange JR, Langstein HN, et al. Evidence for IFN-gamma as a mediator of the lethality of endotoxin and tumor necrosis factor-alpha. J Immunol. 1992;149:1666–1670.

[44] Echtenacher B, Falk W, Männel DN, et al. Requirement of endo-genous tumor necrosis factor/cachectin for recovery from experi-mental peritonitis. J Immunol. 1990;145(11):3762–3766.

[45] Marino MW, Dunn A, Grail D, et al. Characterization of tumor necrosis factor-deficient mice. Proceedings of the National Academy of Sciences of the United States of America 1997; 94:8093–8098.

[46] Netea MG, Kullberg BJ, Joosten LA, et al. Lethal Escherichia coli and Salmonella typhimurium endotoxemia is mediated through different pathways. Eur J Immunol. 2001;31(9):2529–2538.

[47] Rothe J, Lesslauer W, Lötscher H, et al. Mice lacking the tumour necrosis factor receptor 1 are resistant to TNF-mediated toxicity but highly susceptible to infection by Listeria monocytogenes. Nature. 1993;364(6440):798–802.

[48] Steeland S, Ryckeghem SV, Vandewalle J, et al. Simultaneous inhibition of tumor necrosis factor receptor 1 and matrix metal-loproteinase 8 completely protects against acute inflammation and sepsis. Crit Care Med. 2018;46:e67–75.

[49] Taniguchi T, Takata M, Ikeda A, et al. Failure of germinal center formation and impairment of response to endotoxin in tumor necrosis factor alpha-deficient mice. Lab Invest. 1997;77:647–658.

[50] Vandenbroucke RE, Dejonckheere E, Hauwermeiren FV, et al. Matrix metalloproteinase 13 modulates intestinal epithelial barrier integrity in inflammatory diseases by activating TNF. Embo Mol Med. 2013;5(7):1000–1016.

[51] Vandewalle J, Steeland S, Ryckeghem SV, et al. A study of cecal ligation and puncture-induced sepsis in tissue-specific tumor necrosis factor receptor 1-deficient mice. Front Immunol. 2019;10:2574.

[52] Marshall JC Why have clinical trials in sepsis failed? Trends Mol Med. 2014;20:195–203.

[53] Kihara A, Kabeya Y, Ohsumi Y, et al. Beclin–phosphatidylinositol 3-kinase complex functions at the trans-Golgi network. Embo Rep. 2001;2(4):330–335.

[54] Liang XH, Jackson S, Seaman M, et al. Induction of autophagy and inhibition of tumorigenesis by beclin 1. Nature. 1999;402:672–676.

[55] Matsunaga K, Saitoh T, Tabata K, et al. Two Beclin 1-binding proteins, Atg14L and Rubicon, reciprocally regulate autophagy at different stages. Nat Cell Biol. 2009;11:385–396.

[56] Zhong Y, Wang QJ, Li X, et al. Distinct regulation of autophagic activity by Atg14L and Rubicon associated with Beclin 1–phosphatidylinositol-3-kinase complex. Nat Cell Biol. 2009;11 (4):468–476.

[57] Chen S, Wang C, Yeo S, et al. Distinct roles of autophagy-dependent and -independent functions of FIP200 revealed by generation and analysis of a mutant knock-in mouse model. Genes Dev. 2016;30:856–869.

[58] Nishimura T, Kaizuka T, Cadwell K, et al. FIP200 regulates targeting of Atg16L1 to the isolation membrane. Embo Rep. 2013;14:284–291.

[59] Henault J, Martinez J, Riggs JM, et al. Noncanonical autophagy is required for type I interferon secretion in response to DNA-immune complexes. Immunity. 2012;37:986–997.

[60] Diao J, Liu R, Rong Y, et al. ATG14 promotes membrane tether-ing and fusion of autophagosomes to endolysosomes. Nature. 2015;520:563–566.

[61] Liu R, Zhi X, Zhong Q ATG14 controls SNARE-mediated auto-phagosome fusion with a lysosome. Autophagy. 2015;11:847–849.

[62] Saitoh T, Fujita N, Jang MH, et al. Loss of the autophagy protein Atg16L1 enhances endotoxin-induced IL-1β production. Nature. 2008;456(7219):264–268. DOI:10.1038/nature07383

[63] Shi C-S, Shenderov K, Huang N-N, et al. Activation of autophagy by inflammatory signals limits IL-1β production by targeting ubiquitinated inflammasomes for destruction. Nat Immunol. 2012;13:255–263.

[64] Glaccum MB, Stocking KL, Charrier K, et al. Phenotypic and functional characterization of mice that lack the type I receptor for IL-1. J Immunol. 1997;159(7):3364–3371.

[65] Lamkanfi M, Sarkar A, Walle LV, et al. Inflammasome-Dependent release of the alarmin HMGB1 in endotoxemia. J Immunol. 2010;185(7):4385–4392.

[66] Lamkanfi M, Moreira LO, Makena P, et al. Caspase-7 deficiency protects from endotoxin-induced lymphocyte apoptosis and improves survival. Blood. 2009;113(12):2742–2745.

[67] Li P, Allen H, Banerjee S, et al. Mice deficient in IL-1β-converting enzyme are defective in production of mature IL-1β and resistant to endotoxic shock. Cell. 1995;80(3):401–411.

[68] Netea MG, Fantuzzi G, Kullberg BJ, et al. Neutralization of IL-18 reduces neutrophil tissue accumulation and protects mice against lethal escherichia coli and salmonella typhimurium endotoxemia. J Immunol. 2000;164(5):2644–2649.

[69] Berghe TV, Demon D, Bogaert P, et al. Simultaneous targeting of IL-1 and IL-18 is required for protection against inflammatory and septic shock. Am J Respir Crit Care Med. 2014;189:282–291.

[70] Wang S, Miura M, Jung YK, et al. Murine caspase-11, an ICE-interacting protease, is essential for the activation of ICE. Cell. 1998;92(4):501–509.

[71] Man SM, Karki R, Briard B, et al. Differential roles of caspase-1 and caspase-11 in infection and inflammation. Sci Rep. 2017;7:45126.

[72] Bucklin SE, Russell SW, Morrison DC Augmentation of anti-cytokine immunotherapy by combining neutralizing monoclonal antibodies to interferon-γ and the interferon-γ receptor: protec-tion in endotoxin shock. J Endotoxin Res. 2016;1(1):45–51.

[73] Heinzel FP The role of IFN-gamma in the pathology of experi-mental endotoxemia. J Immunol. 1990;145:2920–2924.

[74] Heremans H, Damme JV, Dillen C, et al. Interferon gamma, a mediator of lethal lipopolysaccharide-induced Shwartzman-like shock reactions in mice. J Exp Med. 1990;171:1853–1869.

[75] Wilson CB, Ray M, Lutz M, et al. The RON receptor tyrosine kinase regulates IFN-γ production and responses in innate immu-nity. J Immunol. 2008;181(4):2303–2310.

[76] Schroder K, Hertzog PJ, Ravasi T, et al. Interferon-γ: an overview of signals, mechanisms and functions. J Leukoc Biol. 2004;75 (2):163–189.

[77] Marino MW, Dunn A, Grail D, et al. Characterization of tumor necrosis factor-deficient mice. Proceedings of the National Academy of Sciences of the United States of America 1997;94:8093–8098.

[78] Beutler B, Milsark IW, Cerami AC Passive immunization against cachectin/tumor necrosis factor protects mice from lethal effect of endotoxin. Science. 1985;229:869–871.

[79] Abram CL, Roberge GL, Hu Y, et al. Comparative analysis of the efficiency and specificity of myeloid-Cre deleting strains using ROSA-EYFP reporter mice. J Immunol Methods. 2014;408:89–100.

[80] Roberts AW, Popov LM, Mitchell G, et al. Cas9+ conditionally-immortalized macrophages as a tool for bacterial pathogenesis and beyond. Elife. 2019;8:1287.

[81] Dinarello CA, Novick D, Kim S, et al. Interleukin-18 and IL-18 binding protein. Front Immunol. 2013;4:289.

[82] Murray RZ, Stow JL Cytokine secretion in macrophages: sNAREs, rabs, and membrane trafficking. Front Immunol. 2014;5:538.

[83] Gentle IE Supramolecular complexes in cell death and inflamma-tion and their regulation by autophagy. Front Cell Dev Biol. 2019;7:73.

[84] Gurung P, Malireddi RKS, Anand PK, et al. Toll or interleukin-1 receptor (TIR) domain-containing adaptor inducing interferon-β (TRIF)-mediated caspase-11 protease production integrates Toll-like receptor 4 (TLR4) protein- and Nlrp3 inflammasome-mediated host defense against enteropathogens. J Biol Chem. 2012;287:34474–34483.

[85] Rathinam VAK, Vanaja SK, Waggoner L, et al. Trif licenses caspase-11-dependent nlrp3 inflammasome activation by gram-negative bacteria. Cell. 2012;150(3):606–619.

[86] Mandal P, Feng Y, Lyons JD, et al. Caspase-8 collaborates with caspase-11 to drive tissue damage and execution of endotoxic shock. Immunity. 2018;49(1):42–55.e6. DOI:10.1016/j.immuni.2018.06.011

[87] Kimura T, Watanabe E, Sakamoto T, et al. Autophagy-Related IRGM polymorphism is associated with mortality of patients with severe sepsis. PLoS One. 2014;9:e91522.

[88] Savva A, Plantinga TS, Kotanidou A, et al. Association of autophagy-related 16-like 1 (ATG16L1) gene polymorphism with sepsis severity in patients with sepsis and ventilator-associated pneumonia. Eur J Clin Microbiol Infect Dis. 2014;33:1609–1614.

[89] Shao Y, Chen F, Chen Y, et al. Association between genetic polymorphisms in the autophagy-related 5 gene promoter and the risk of sepsis. Sci Rep. 2017;7:9399.

[90] Tesi B, Bryceson YT Hlh: genomics illuminates pathophysiological diversity. Blood. 2018;132:5–7.

[91] Rosshart SP, Herz J, Vassallo BG, et al. Laboratory mice born to wild mice have natural microbiota and model human immune responses. Science. 2019;365:eaaw4361.

[92] Channappanavar R, Fehr AR, Vijay R, et al. Dysregulated type i interferon and inflammatory monocyte-macrophage responses cause lethal pneumonia in SARS-CoV-infected mice. Cell Host & Microbe. 2016;19:181–193.

[93] Shi X, Zhou W, Huang H, et al. Inhibition of the inflammatory cytokine tumor necrosis factor-alpha with etanercept provides protection against lethal H1N1 influenza infection in mice. Crit Care. 2013;17:R301–9.

[94] Karki R, Sharma BR, Tuladhar S, et al. Synergism of TNF-α and IFN-γ triggers inflammatory cell death, tissue damage, and mortality in SARS-CoV-2 infection and cytokine shock syndromes. Cell. 2021;184(1):149–168.e17. DOI:10.1016/j.cell.2020.11.025

[95] Hara T, Nakamura K, Matsui M, et al. Suppression of basal autophagy in neural cells causes neurodegenerative disease in mice. Nature. 2006;441:885–889.

[96] DeSelm CJ, Miller BC, Zou W, et al. Autophagy proteins regulate the secretory component of osteoclastic bone resorption. Dev Cell. 2011;21:966–974.

[97] Hwang S, Maloney NS, Bruinsma MW, et al. Nondegradative role of Atg5-Atg12/Atg16L1 autophagy protein complex in antiviral activity of interferon gamma. Cell Host & Microbe. 2012;11 (4):397–409. DOI:10.1016/j.chom.2012.03.002

[98] Gan B, Peng X, Nagy T, et al. Role of FIP200 in cardiac and liver development and its regulation of TNFα and TSC–mTOR signaling pathways. J Cell Biol. 2006;175(1):121–133.

[99] Gawriluk TR, Hale AN, Flaws JA, et al. Autophagy is a cell survival program for female germ cells in the murine ovary. Reproduction. 2011;141:759–765.

[100] Clausen BE, Burkhardt C, Reith W, et al. Conditional gene targeting in macrophages and granulocytes using LysMcre mice. Transgenic Res. 1999;8:265–277.

[101] Stranges PB, Watson J, Cooper CJ, et al. Elimination of antigen-presenting cells and autoreactive T cells by Fas contributes to prevention of autoimmunity. Immunity. 2007;26:629–641.

[102] Passegué E, Wagner EF, Weissman IL JunB deficiency leads to a myeloproliferative disorder arising from hematopoietic stem cells. Cell. 2004;119:431–443.

[103] Huang S, Hendriks W, Althage A, et al. Immune response in mice that lack the interferon-γ receptor. Science. 1993;259 (5102):1742–1745.

[104] Wang GG, Calvo KR, Pasillas MP, et al. Quantitative production of macrophages or neutrophils ex vivo using conditional Hoxb8. Nat Methods. 2006;3:287–293.

[105] Amend SR, Valkenburg KC, Pienta KJ Murine hind limb long bone dissection and bone marrow isolation. J Vis Exp JoVe. 2016;53936.

[106] Maculins T, Verschueren E, Hinkle T, et al. Multiplexed proteomics of autophagy-deficient murine macrophages reveals enhanced antimicrobial immunity via the oxidative stress response. Elife. 2021;10:e62320.